

Magnetic properties of zinc substituted cobalt ferrite thin films synthesized by the sol-gel process

LE-ZHONG LI^{*a}, ZHI-YONG PU^b, RUI WANG^a, XIAO-XI ZHONG^a, XIAO-QIANG TU^a, LONG PENG^a

^aSichuan Province Key Laboratory of Information Materials and Devices Application, Chengdu University of Information Technology, Chengdu 610225, Sichuan, People's Republic of China

^bState Key Laboratory of Electronic Thin Films and Integrated Devices, University of Electronic Science and Technology of China, Chengdu 610054, China

Zn-substituted Co ferrite thin films, $\text{Co}_{1-x}\text{Zn}_x\text{Fe}_2\text{O}_4$ ($0 \leq x \leq 1.0$), were synthesized by the sol-gel process. The variation of magnetocrystalline anisotropy constant obtained by Law of Approach to saturation and static magnetic properties of Zn-substituted Co ferrite thin films have been investigated. The magnetocrystalline anisotropy constant decreased with the increase of Zn substitution. The saturation magnetization increased with the increase of Zn substitution when $x \leq 0.20$, and decreased when $x > 0.20$. Meanwhile, the coercivity initially decreased with the increase of Zn substitution when $x \leq 0.60$, and increased when $x > 0.60$.

(Received November 19, 2015; accepted April 5, 2016)

Keywords: Co ferrite thin films, The sol-gel process, Zn substitution, Magnetocrystalline anisotropy constant, Magnetic property

1. Introduction

Spinel ferrites, MFe_2O_4 , are technologically important group of materials due to their enhanced magnetic and electrical properties. These properties make them very attractive for a variety of applications including but not limited to use as electrodes in energy storage devices, as catalysts, in magnetic storage devices, etc. [1–8].

It is well known that the ferrites MFe_2O_4 with the spinel structure are based on a face-center cubic lattice of the oxygen ions. Each spinel unit cell contains eight formula units. In each unit cell, there are 64 tetrahedral sites (A sites) and 32 octahedral sites (B sites). Therefore, the chemical, structural, and magnetic properties of ferrite are strongly influenced by their composition and microstructure, which are sensitive to the preparation methodologies [9]. They show various magnetic properties depending on the cation distribution. Various cations can be placed in the structure of AB_2O_4 in A site and B site can result in the interesting physical and chemical properties in spinel ferrites [10].

The trend for downsizing electronic equipments and the potential applications of soft ferrite materials have lead to the fabrication of thin films of ferrites. And the ferrite thin films have been prepared by different techniques: sol-gel [11–14], spin spray plating [15–17], magnetron sputtering [18], pulsed-laser deposition [19], etc. The sol-gel method adopted in this paper has the following advantages [20]. First, the composition of films trends to be homogeneous and films possess high quality. Second, the heat treatment temperature is low, and the

microstructure and microcrystallite size of thin films can be controlled by the annealing temperature. Last, the equipment is cheap and the high vacuum is not necessary.

Co-ferrite thin films with high coercivity have a significant potential in many applications including magnetic recording, magneto-optical recording, and microelectromechanical system devices [21–25]. There are a few reports on the properties of Zn substituted Co ferrite nanoparticles [26–32]. But to our knowledge, there are few reports on the Zn-substituted Co ferrite thin films synthesized by the sol-gel process. Therefore, in this paper we investigated the variation of magnetocrystalline anisotropy constant obtained by Law of Approach to saturation (LoAS) and static magnetic properties of Zn-substituted Co ferrite thin films.

2. Experimental procedures

The samples of $\text{Co}_{1-x}\text{Zn}_x\text{Fe}_2\text{O}_4$ ($x=0, 0.20, 0.40, 0.60, 0.80, 1.0$) ferrite thin films were synthesized by the sol-gel process. Stoichiometric quantities of analytical grade $\text{Zn}(\text{CH}_3\text{COO})_2 \cdot 2\text{H}_2\text{O}$, $\text{Co}(\text{NO}_3)_2 \cdot 6\text{H}_2\text{O}$ and $\text{Fe}(\text{NO}_3)_3 \cdot 9\text{H}_2\text{O}$ were first dissolved in 2-methoxyethanol to form a mixed solution. After the solution was stirred for 1 h, the acetic acid was added to adjust the concentration of the solution to 0.3mol/L. Meanwhile, polyethylene glycol was added. As a kind of surfactant, it can effectively prevent the colloidal particles of chelate from being jointed with each other. Then, the prepared solution was continuously stirred for 2 h and placed at room

temperature for 36 h to form the stable sol-gel precursors used for the following processes. First, the wet films were deposited by a spin coating method on the substrate of Si (111) at 4000 rpm for 30 s. Second, the wet films were dried at 200°C for 10 min to remove the mixed solvents. Third, the operation of spin coating and drying was repeated to get the required thickness of the films. Last, the dried films were heated at 400 °C for 30 min to pyrolyze and exclude the organic substances and then were annealed at 800 °C for 1h in air and cooled slowly in the furnace.

The static magnetic measurements by the TOEI VSM-5S-15 vibrating sample magnetometer (VSM) at room temperature.

3. Results and discussion

3.1. Magnetocrystalline anisotropy constant

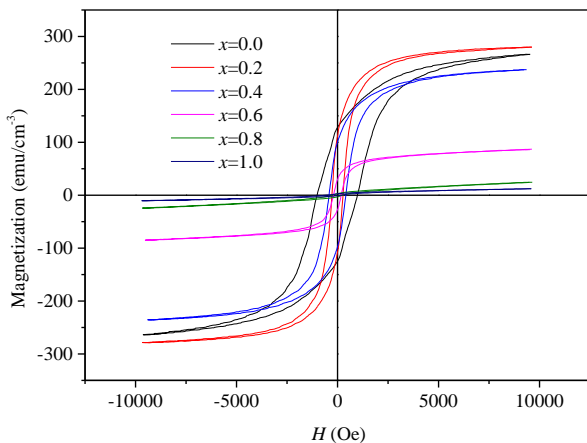


Fig. 1. Hysteresis loops of CoZn ferrite thin films

Fig. 1 shows the hysteresis loops of $\text{Co}_{1-x}\text{Zn}_x\text{Fe}_2\text{O}_4$ ($0 \leq x \leq 1.0$) ferrite thin films. The high-field region of the hysteresis loops can be modeled using the Law of Approach to saturation (LoAS) based on the assumption that at sufficiently high field only domain rotational processes remain, with an additional forced magnetization term that is linear with applied field [33–35]. In order to evaluate the variation of the magnetocrystalline anisotropy constant, it is assumed that all irreversible hysteretic processes are completed when the major hysteresis loop closed and that further increase of the magnetic moment is due to domain rotational processes which are connected with the magnetic anisotropy [33, 34]. Based on the Law of Approach to saturation (LoAS), which describes the dependence of magnetization (M) on the applied field (H) for $H \gg H_c$, magnetization near the saturation magnetization, M_s can be experimentally obtained by the well-known empirical formula [34]

$$M = M_s \left(1 - \frac{a}{H} - \frac{b}{H^2} - \dots \right) + \kappa H \quad (1)$$

where M_s and H are the saturation magnetization and applied field, respectively, and κH is the forced magnetization term [35]. The coefficient $a \approx 0$ in the high field region as it is related to domain wall pinning. For cubic structured anisotropic polycrystalline materials, the coefficient b is given by [34, 35]

$$b = \frac{8}{105} \frac{K_1^2}{\mu_0^2 M_s^2} \quad (2)$$

The numerical coefficient 8/105 is for random polycrystalline specimens with cubic anisotropy, μ_0 is the permeability of free space, and K_1 is the cubic magnetocrystalline anisotropy constant. The high-field regime ($0.97M_s < M \leq M_s$) of the major hysteresis curves are fitted using the standard LoA approach by Eqs. (1) and (2). Detailed examination of the curves revealed that forced magnetization (κH) is negligible in this regime, as might be expected. Therefore, M_s and K_1 are the only fitting parameters when $\kappa=0$.

The variation of the calculated magnetocrystalline anisotropy constant with different Zn substitution is shown in Fig. 2. The results indicate that K_1 decreases with the increase of Zn substitution. According to the one-ion theory model, the ground state of Zn^{2+} ($3d^{10}$) which indicates that the Zn^{2+} ion is nonmagnetic ion. So, with the increase of Zn substitution the magnetocrystalline anisotropy field decreases. Eventually, K_1 decreases with the increase of Zn substitution.

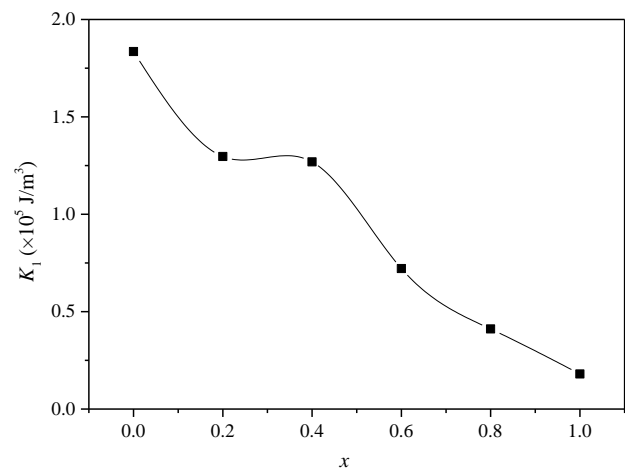


Fig. 2. Variation of K_1 with different Zn substitution (x)

3.2. Static magnetic properties

Fig. 3 shows the saturation magnetization (M_s) and coercivity (H_c) of thin films as a function of Zn substitution (x). The saturation magnetization (M_s)

initially increases with the increase of Zn substitution when $x \leq 0.20$, and decreases when $x > 0.20$. Meanwhile, the coercivity (H_c) initially decreases with the increase of Zn substitution when $x \leq 0.60$, and increases when $x > 0.60$. M_s reaches the maximum (279.8 emu/cm^3) with Zn substitution (x) is 0.20. And H_c reaches the minimum (179.0 Oe) with Zn substitution (x) is 0.60.

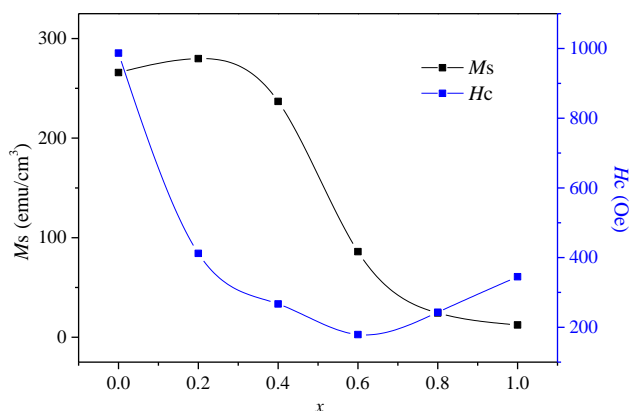


Fig. 3. M_s and H_c of $\text{Co}_{1-x}\text{Zn}_x\text{Fe}_2\text{O}_4$ ferrite thin films

Magnetic properties of ferrites are sensitively dependent on the structure, composition, defects, crystallite size, internal strain and cation distribution.

It is well known that there are two sites, A (tetragonal) and B (octahedral), in the spinel ferrite. According to Néel's two sublattice model of ferrimagnetisms [36], the magnetic moment is given by $M = |M_B - M_A|$, where M_A and M_B are the magnetizations of A and B-sites respectively. So, the initial increase of M_s is attributed to the M_A decreases with Zn^{2+} substitution which is due to the nonmagnetic Zn^{2+} ion preferentially occupies A sites in the spinel ferrite and displaces Fe^{3+} ion from A sites to B sites. Superexchange interactions between the two magnetic cations via an intermediate oxygen ion in the spinel structure can occur as a result of intra-sublattice AA and BB interactions and inter-sublattice AB interactions. The strength of the superexchange interactions depends on the angle and distance between the two metal cations. And among them AB interaction is the strongest one and AA interaction is the weakest one [36]. Therefore, AB interaction becomes weaker because the magnetic ions decrease in A-site with the further increase of Zn substitution, which results in the YK angles (θ_{YK}) increase based on the three sub-lattice model suggested by Yafet-Kittel (YK) [37]. The increase of θ_{YK} can lead to the magnetic moments become more unparallelled, and M_B decreases. Eventually, M_s decreases when Zn substitution (x) exceeds 0.2. For ZnFe_2O_4 ($x=1.0$), θ_{YK} is 90° indicating that it is a collinear antiferromagnet [38]. Therefore, there is a little M_s value (12.3 emu/cm^3) with strong magnetic field when $x=1.0$

The coercivity (H_c) of ferrite thin films as a function

of Zn substitution (x) is shown in Fig. 3 which indicates that H_c gradually decreases with the increase of Zn substitution when $x \leq 0.60$, and increases when $x > 0.60$. The decrease of H_c with Zn substitution $x \leq 0.60$ mainly due to the nonmagnetic Zn^{2+} ions substitution decrease the magnetocrystalline anisotropy energy which can be confirmed by the decrease of the magnetocrystalline anisotropy constant (K_1). However, H_c increases with the further increase of Zn substitution when $x > 0.60$, although K_1 decrease. In fact, ZnFe_2O_4 is an antiferromagnetic ferrite, and consequently the excessive Zn substitution results in the ferrimagnetic thin films gradually changes to antiferromagnet which make the films hardly magnetize. So, H_c increases with Zn substitution when $x > 0.60$.

4. Conclusions

Zn-substituted Co ferrite thin films, $\text{Co}_{1-x}\text{Zn}_x\text{Fe}_2\text{O}_4$ ($0 \leq x \leq 1.0$), have been synthesized by the sol-gel method. The variation of magnetocrystalline anisotropy constant and static magnetic properties of thin films have been investigated and the following results have been obtained:

(1) The magnetocrystalline anisotropy constant obtained by Law of Approach to saturation decreased with the increase of Zn substitution.

(2) The saturation magnetization increased with the increase of Zn substitution when $x \leq 0.20$, and decreased when $x > 0.20$. Meanwhile, the coercivity initially decreased with the increase of Zn substitution when $x \leq 0.60$, and increased when $x > 0.60$.

Acknowledgments

This work was supported by the National Natural Science Foundation of China (Grant No. 51502025).

References

- [1] S. F. Neues, M. W. E. Berg, W. Grunert, et al., J. Am. Chem. Soc. **127**, 12028 (2005).
- [2] S. Sun, C. B. Murray, D. Weller, et al., Science **287**, 1989 (2000).
- [3] A. J. Zarur, J. Y. Ying, Nature **403**, 65 (2000).
- [4] Q. Song, Z. J. Zhang, J. Am. Chem. Soc. **126**, 6164 (2004).
- [5] T. Hyeon, S. S. Lee, J. Park, et al., J. Am. Chem. Soc. **123**, 12798 (2001).
- [6] C. R. Vestal, Q. Song, Z. J. Zhang, J. Phys. Chem. B **108**, 18222 (2004).
- [7] J. Shi, S. Gider, K. Babcock, D. D. Awschalom, Science **271**, 937 (1996).
- [8] M. Sertkol, Y. Köseoğlu, A. Baykal, et al., J. Alloys Compd. **486**, 325 (2009).
- [9] F. Li, J. J. Liu, D. G. Evans, et al., Chem. Mater. **16**, 1597 (2004).
- [10] S. T. Alone, S. E. Shirsath, R. H. Kadam, et al., J.

- Alloys Compd. **509**, 5055 (2011).
- [11] A. S. Albuquerque, J. D. Ardisson, W. Macedo, J. Magn. Mater. **192**, 277 (1999).
- [12] F. Liu, T. L. Ren, C. Yang, et al., Mater. Lett. **60**, 1403 (2006).
- [13] L. Li, R. Wang, X. Tu, et al., J. Magn. Mater. **355**, 306 (2014).
- [14] P. Gao, E. V. Rebrov, T. Verhoeven, et al., J. Appl. Phys. **107**(1–8), 044317 (2010).
- [15] N. Matsushita, T. Nakamura, M. Abe, J. Appl. Phys. **93**, 7133 (2003).
- [16] C. M. Fu, H. S. Hsu, Y. C. Chao, et al., J. Appl. Phys. **93**, 7127 (2003).
- [17] T. H. Hai, H. Van, T. Phong, et al., Physica B, **327**, 194 (2003).
- [18] M. Desai, S. Prasad, N. Venkataramani, et al., J. Appl. Phys. **91**, 7592 (2002).
- [19] C. N. Chinnasamy, S. D. Yoon, A. Yang, et al., J. Appl. Phys. **101**(1–3), 09M517 (2007).
- [20] K. Sun, Z. W. Lan, Z. Yu, et al., Curr. Appl. Phys. **11**, 472 (2011).
- [21] B. X. Gu, Appl. Phys. Lett. **82**, 3707 (2003).
- [22] J. G. Lee, J. Y. Park, Y. J. Oh, et al., J. Appl. Phys. **84**, 2801 (1998).
- [23] M. L. Kahn, Z. J. Zhang, Appl. Phys. Lett. **78**, 3651 (2001).
- [24] A. Lisfi, C. M. Williams, J. Appl. Phys. **93**, 8143 (2003).
- [25] Y. C. Wang, J. Ding, J. B. Yi, et al., Appl. Phys. Lett. **84**, 2596 (2004).
- [26] L. Wang, F. -S. Li, Chin. Phys. B **17**, 1858 (2008).
- [27] S. Urcia-Romero, O. Perales-Pérez, O. N. C. Uwakweh, et al., J. Appl. Phys. **109**(1–3), 07B512 (2011).
- [28] R. Arulmurugan, G. Vaidyanathan, et al., Physica B: Condensed Matter. **363**, 225 (2005).
- [29] R. Arulmurugan, B. Jeyadevan, G. Vaidyanathan, et al., J. Magn. Mater. **288**, 470 (2005).
- [30] M. Mozaffari, S. Manouchehri, M.H. Yousefi, et al., J. Magn. Mater. **322**, 383 (2010).
- [31] G. A. Petitt, D. W. Forester, Phys. Rev. **B 4**, 3912 (1971).
- [32] P. B. Pandya, H. H. Joshi, R. G. Kulkarni, J. Mater. Sci. **26**, 5509 (1991).
- [33] B. D. Cullity, C. D. Graham, Introduction to magnetic materials, IEEE Press, Piscataway, 2011.
- [34] W. D. Zhong, Ferromagnetism, Science Press, Beijing, 1998.
- [35] M. J. Iqbal, Z. Ahmad, T. Meydan, et al., J. Appl. Phys. **111**, 033906 (1–7) (2012).
- [36] D. F. Wan, X. L. Ma, The Physics of Magnetism, UESTC Press: Chengdu, 1994.
- [37] Y. Yafet, C. Kittel, Phys. Rev. **87**, 290 (1952).
- [38] N. S. Satya Murthy, M. G. Natera, S. I. Youssef, et al., Phys. Rev. **181**, 969 (1969).

*Corresponding author: lezhongli@cuit.edu.cn